BBA - Biomembranes 1863 (2021) 183494

Contents lists available at ScienceDirect

BBA - Biomembranes

journal homepage: www.elsevier.com/locate/bbamem

The influence of lipid membranes on fluorescent probes' optical properties

Silvio Osella [a,*], Stefan Knippenberg [b,c,d,*]

[a] Biological Systems Simulation Lab, Centre of New Technologies, University of Warsaw, Banacha 2C, 02-097 Warsaw, Poland
[b] Regional Centre of Advanced Technologies and Materials, Department of Physical Chemistry, Faculty of Science, Palacký University Olomouc, 17. listopadu 12, 771 46 Olomouc, Czech Republic
[c] Department of Theoretical Chemistry and Biology, School of Engineering Sciences in Chemistry, Biotechnology and Health, KTH Royal Institute of Technology, SE-10691 Stockholm, Sweden
[d] Theoretical Physics, Hasselt University, Agoralaan Building D, 3590 Diepenbeek, Belgium

ARTICLE INFO

Keywords:
QM/MM
Lipid bilayer
Non-linear optics
Absorption
Fluorescence
Fluorescence anisotropy

ABSTRACT

Background: Organic fluorophores embedded in lipid bilayers can nowadays be described by a multiscale computational approach. Combining different length and time scales, a full characterization of the probe localization and optical properties led to novel insight into the effect of the environments.
Scope of review: Following an introduction on computational advancements, three relevant probes are reviewed that delineate how a multiscale approach can lead to novel insight into the probes' (non) linear optical properties. Attention is paid to the quality of the theoretical description of the optical techniques.
Major conclusions: Computation can assess a priori novel probes' optical properties and guide the analysis and interpretation of experimental data in novel studies. The properties can be used to gain information on the phase and condition of the surrounding biological environment.
General significance: Computation showed that a canonical view on some of the probes should be revisited and adapted.

1. Introduction

In the last few years, increased attention has been paid to the use of computational power and molecular modelling to tackle complex problems in biological environments, such as the behaviour of fluorescent probes in lipid bilayers. The classical approach is to assess the localization of the probes embedded in model membranes composed of one or more kinds of lipids by molecular dynamics (MD) methods. In this way, it is possible to know with high accuracy the localization of probes in the bilayers, and a wealth of studies in literature reported the success of this computational approach [1–6]. Yet, an important part of the analysis cannot be reached within this methodology, namely the study of the optical properties of these probes while embedded in the membranes, for which quantum mechanical (QM) calculations are needed. This is an important key point in the experimental characterization of the membrane phase, and the knowledge of it is essential to determine the health or illness of a cell. In fact, depending on the phase of the membrane it is possible to assess the nature of the cell [7]. Depending on the amount of cholesterol, its malignant or benign character can be discussed. Experimentally, this can be accessed by the use of different spectroscopic techniques which take advantage of the anisotropy of the environment and its effect over the optical properties of the embedded probe [8,9]. Yet, little computational studies have been reported in literature regarding this topic, despite the strong insight they could provide not only on the design of novel probes, but also with respect to the assessment of different optical properties of existing probes, with the aim of obtaining a universal probe.

This is even more striking considering that nowadays this issue can be assessed by the use of hybrid quantum mechanics/molecular mechanics (QM/MM) approaches, which allow to consider the probe at a high ab initio level and the rest of the environment, in its first approximation, as point charges. Despite the introduction of the QM/MM methods to study complex systems in the early 2000nd [10], little literature is present on the effect of anisotropic biological environment on the optical properties of organic fluorophores. The improvement of computational clusters eventually allowed computational simulations to be an active part in this research field, also thanks to the use of multiscale approaches: a large model system, which comprises the probe immersed into the lipid bilayer, can be studied by means of extensive MD simulations, which even allow the analysis of nanodomains by

* Corresponding authors.
E-mail addresses: s.osella@cent.uw.edu.pl (S. Osella), stefan.knippenberg@uhasselt.be (S. Knippenberg).

https://doi.org/10.1016/j.bbamem.2020.183494
Received 20 June 2020; Received in revised form 13 October 2020; Accepted 15 October 2020
Available online 29 October 2020

resorting to simulation times up to μs. Then, the QM/MM approach allows a smaller portion of the system to be considered and treated at a higher level of accuracy in order to study the optical properteis of the probe when embedded in a complex biological environment.

In this context, we developed over the years a methodology to fully characterize different probes in view of their different positions, orientations, conformational versatilities and optical properties when embedded in model bilayers. In this paper, three prominent sets of probes are presented and the accepted view of how they should behave in a membrane is challenged, which might be seen as controversial. Nevertheless, we will show not only how computational simulations can explain particular experimental findings by analyzing the localization and orientation of probes in different membrane phases, but also how computation can uncover novel functionalities of well-used probes by reverting to a multiscale approach.

First, we focus on Laurdan, which is a widely known and commonly used probe in fluorescence microscopy, to validate our computational approach (validation step). We discuss its strong properties and critically evaluate a probe which was initially advocated as an improvement of Laurdan. We discover that Laurdan has two conformers whose optical properties are clearly different, which urges to change the accepted view on this probe. In the next section, we focus on rather rigid probes and predict that the experimental observation of their (non) linear optical properties is sufficient to identify and discriminate different membrane phases (soundness step). In the last section, the obtained experience and developed techniques are used to investigate membrane probes which are derived from archetype conformationally flexible azobenzene molecules (prediction step).

2. Laurdan: a novel view upon an old probe

Laurdan is one of the most used and studied probes as it is the archetype of solvatochromic probes [11]. This class of molecules change their optical properties depending on the polarity of the environment they are immersed in, due to a change in their dipole moment upon excitation. When embedded in a lipid bilayer, different phases lead to different response to optical properties, such as absorption and two-photon cross section [12]. Despite its wide use, Laurdan does not have a specific orientation in the membrane, as it lacks a strong functional group which can strongly interact with the amphiphilic membrane head and 'lock' it in a single position [13]. This introduced some controversy over the years on the evaluation of experimental data, with a large variation of results depending on experimental conditions [14–20]. In order to remove this uncertainty, variants, such as C-Laurdan which present a carbonyl group which can efficiently interact with the membrane head [21], have been synthesised.

MD simulations of the two probes in a DOPC (Ld) membrane have shown that the carboxylic group of C-Laurdan is responsible for a strong interaction between C-Laurdan and the head groups of DOPC. It leads to a closer proximity to the membrane surface, with a distance of 1.60 nm from the bilayer center, while for Laurdan it is at 1.24 nm (Fig. 1c). Due to this strong interaction, a high rigidity has been obtained, with orientation (considering the transition dipole moment) of 53° with respect to the bilayer normal (Fig. 1a). This is different for Laurdan, which is not anchored to the membrane and has more freedom of movement. It can access many different orientations, with a tilt angle ranging from 70 to 100°, which explains the uncertainty over its position observed in experiments [13]. The QM/MM analysis of the absorption properties provide additional evidence of the differences between the two probes. Analyzing the absorption spectrum composed through the selected snapshots, a high rotational freedom has been seen for Laurdan in DOPC, while a more restrained spread was found for C-Laurdan, reflecting the hindered cradling motion of the probe around its main orientation. An intense Stokes shift of 60–80 nm has been found, with strong variation for Laurdan due to the high rotational freedom in DOPC, while a more restrained spread has been found for C-Laurdan, reflecting the hindered wobbling of the probe. Moreover, fluorescence anisotropy confirms the higher rotational motion of Laurdan with

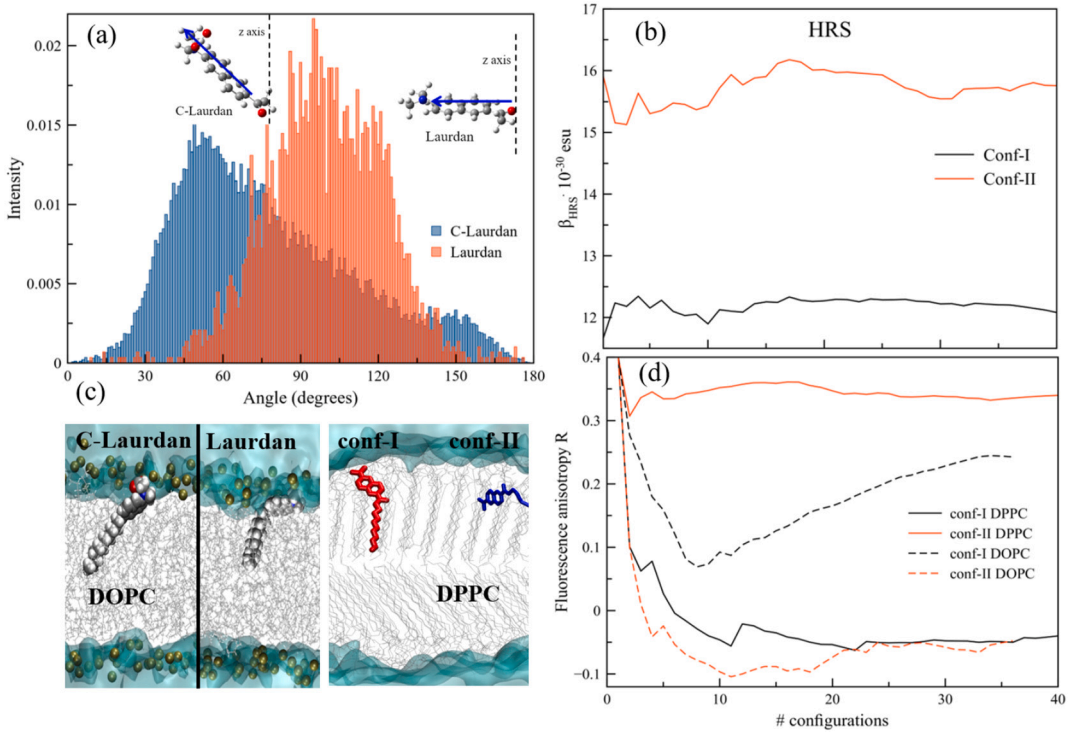

Fig. 1. (a) Difference in transition dipole moment orientation of Laurdan and C-Laurdan in DOPC (Ld). The transition dipole moment vector is depicted as blue arrow; (b) HRS optical response of the two conformers in DPPC; (c) representative localization of C-Laurdan and Laurdan in DOPC and of the two conformers of Laurdan in DPPC (So); (d) Difference in fluorescence anisotropy for the two conformers of Laurdan in DOPC (Ld) and DPPC (So) membranes. Parts (b) and (d) are reprinted with permission from [12]. Copyright 2019 American Chemical Society.

respect to C-Laurdan, leading to a more confined wobbling motion of the latter compound and hence a more precise location within the DOPC membrane.

A more interesting behaviour appears when Laurdan is embedded in a sterically hindered environment, such as a DPPC membrane in the gel phase (So). Through extensive MD simulations of both conformers embedded in the membrane, we observed a strong difference in their localization, with one conformer assuming an elongate shape (conf-I) and interacting with the membrane head through the amino group, while the second conformer assumes a more 'L-shaped' conformation (conf-II, Fig. 1c) and interacts now with the membrane high density layer of the head groups through the carbonyl group [22]. This is not the case when Laurdan is immersed in a DOPC (Ld) phase, and can be explained considering the difference in hindrance between the two phases; in Ld, the rotation of the carbonyl group around the naphthalene core of Laurdan is allowed, and the nature of the phase itself leads to a coexistence of both conformers with a relatively low rotational energy barrier of 2–3 kcal/mol. In a So phase, the rotation is practically blocked due to the steric hindrance and the drop of the interconversion rate constant linked to the presence of the viscous medium [23,24]. As a result, both conformations can exist, without any intermixing between them. Since no conformational change is found in the 400 ns MD run, we can safely state that the interconversion between Laurdan's conformers will gradually decrease as well in an Lo membrane with increasing amount of Cholesterol. These results can be assessed in upcoming kinetic studies.

These results open to possible different responses to optical stimuli when light is shone on the different membranes. The two conformations coalesce in the Ld phase, while they present different realizations in a So phase; thus, their optical response should differ. Through the analysis of QM/MM calculations on both conformers in DOPC (Ld) and DPPC (So) membranes, we indeed found this different response behaviour [12]. To achieve this, a statistically meaningful amount of independent snapshots have been selected from the MD simulations for both conformers. In the electrostatic embedding, the probe is considered at the TDDFT/CAM-B3LYP level of theory, while the lipids and molecules of the environments are replaced by point charges. A practical problem is the size of the set with snapshots: for linear absorption calculations, the computer time is rather modest, while for the calculation of non-linear optical properties the computational cost for ~40 snapshots might become relatively hard to manage. There is thus a certain trade-off to be considered between the computational time and the number of snapshots to be considered. For the type of spectroscopies here considered, we could verify that convergence is reached starting from 30 snapshots [13]. Yet, this is not universal, and for different probe/environment compositions the convergence of optical properties vs. number of snapshots should be thoroughly checked. The argument of the computational cost and the special requirements on the available hardware in these QM/MM regimes can already be understood when the scaling properties of the codes are considered: MD software packages are generally scalable using MPI formalism over a multitude of nodes, while for many quantum chemical software programs, maximum efficiency is already reached by using all cores which are available in only a few nodes. This means that often the QM/MM calculations are performed on other computational architectures than the MD simulations.

From the QM/MM analysis, we observe that the different orientations of the naphthalene moiety lead to a different orientation of the transition dipole moment (tdm), which is the key factor for optical analyses. We observed a bathochromic shift of 15 nm going from conf-I to conf-II for S_1 in the absorption spectra when the probe is embedded in DPPC, while the two peaks coalesce in DOPC. Already this first result shows the versatility of Laurdan as a molecular rotor, since experimental characterization techniques should be able to screen between the two conformers. To have additional evidence, we performed an analysis based upon non-linear optics and focused on two-photon absorption (TPA) and hyper-Rayleigh scattering (HRS) analyses. From the TPA cross sections of the energetically low lying excited states, we assess which conformer is active (i.e. gives the higher values in Göppert-Mayer [GM]). Due to the different orientation of the probe's head, and consequent difference in tdm orientation, the first excited state is active for conf-II, with cross section values 2.5 times higher than conf-I. The opposite is found for S_3, where now conf-I is the active state, with cross section values twice as high as for conf-II, while S_2 can be considered a dark state for TPA (cross section values lower than 5 GM). This is in strong contrast with the analysis in DOPC, where for both conformers we observed very similar cross section values. HRS also shows a difference in performance for the two conformations when Laurdan is embedded in DPPC, with now conf-II being the active conformer (Fig. 1b).

Finally, we consider the fluorescence properties of Laurdan in the two different membrane phases. To be considered as discernible conformers, the fluorescence intensity, lifetime, or anisotropy should differ in the different environments. From the MD analysis, we obtained two different localization populations of the conformers in DPPC, while this reduces to the same population in DOPC [12]. This means that in DPPC we should have two distinct fluorescence decay times. In fact, we computed that these times amount to 5 ns for conf-II and to 9 ns for conf-I. On the other hand, in DOPC we observe one decay time only, which can be considered as an average over the two conformers. To gain more insight into the fluorescence properties, we computed also the fluorescence anisotropy ratio as $r = (I_{\parallel} - I_{\perp})/(I_{\parallel} + 2I_{\perp})$. A pronounced depolarization is the direct consequence of the ease of intramolecular rotation from conf-I to conf-II in the environment (i.e. Ld phase) while in a more viscous medium like So phase the rotation is hindered and the depolarization is expected to be suppressed. From our analysis we obtained that in DPPC (So) the fluorescence is quickly depolarized for conf-I, while conf-II is not affected by the environment, with a steady anisotropy value close to the reference of 0.4 (Fig. 1d). The strong anisotropy decay confirms the mobility of conf-I with respect to conf-II. Once more, this is not seen in DOPC, where the interconversion between the two conformers is allowed and a strong depolarization is obtained.

As a conclusion, we brought several computational proofs of the different responses to optical stimuli of Laurdan and its conformers when the probe is embedded in different membrane phases: (i) The fluorescence lifetimes of both conformers are clearly different in the So phase, while they are comparable in a more fluid phase. (ii) Strong difference in fluorescence anisotropy decay are computed for both conformers embedded in a viscous medium as DPPC (So). (iii) The reduced packing and increased fluidity of DOPC (Ld) facilitates the rotation and movement of Laurdan and enables conformational changes between Conf-I and Conf-II. (iv) All computational results strongly point to the ability of Laurdan to be a truly versatile probe, which will lead to different response in different environment, thus allowing for membrane phase recognition.

Laurdan is canonically known as a solvatochromic probe: the magnitude of its dipole moment more than doubles after excitation, and, consequently, its spectroscopic properties are prone to solvent relaxation effects. However, since the molecule has two different conformers, we find that Laurdan can also be used as a molecular rotor, which probes the viscosity of the medium. Based on the results of the employed hybrid computational modelling techniques, it is safe to state that the fluorescence intensity, lifetime, and anisotropy between the two different conformations are different in different environments. We hope to encourage experimentalists to consider our findings and to design studies to validate their importance.

At this point, it might be good to review the applied computational approaches and formulate prospects for future computational efforts needed to unravel the photophysical behaviour of Laurdan and investigate the influence on the probe of qualitative differences between surrounding lipid bilayers. An important point for Laurdan as a solvatochromic probe is the effect of solvent polarization and relaxation effects. In the approach used in the studies above, electrostatic embedding has been employed and the water relaxation has essentially been

neglected. Very recently, Baral et al. focused on the Prodan probe, which differs essentially from Laurdan by the absence of the alkyl chain, and put it in a few solvents [25]. Baral et al. used Green's function theory along with the Bethe-Salpeter equation (GW-BSE) to explore the excited state properties of the chromophore. They built an extra loop and coupled the MD calculations with the evolution of the excited state via an iterative update of the charges. Using an electrostatic embedding approach as well, they reported water relaxation times of a few tens of picoseconds. Reverting to the TDDFT theory we used up till now, an analogous approach can be constructed to describe the water relaxation in the neighborhood of Laurdan embedded in a lipid bilayer. Based on Baral's observations and considering the emission lifetimes of Laurdan ranging from a few to approximately 15 ns dependent on the biological environment, it seems now plausible that in a fluorescence study a fully relaxed water layer around the compound is probed.

However, to fully cope with the polarization effects, a study on Laurdan in DPPC or DOPC should be performed using polarizable force fields, while as well iterative loops can be incorporated to update the probe's excited state properties in a second step. At this moment, the computational cost to fulfill this approach to the same extent as the calculations presented in the current study is restrictive, as it is easily multiplied by ten or more when polarizable force fields are used. It might thus be appropriate to select snapshots out of a longer and cheaper MD run, which are then further used in polarizable force field calculations. To move a step further toward a more accurate description of this complex environment, the membrane potential (in the order of 10 meV or more) should be taken into account as an external field.

Another aspect which is expected to have a profound effect on the environment of the probe and in particular the solvent relaxation is the temperature. It is expected that the charge transfer character of the lowest excited state rises at higher temperatures. As a consequence, the relaxation is expected to proceed faster, too [26]. However, kinetically speaking high temperatures might also prevent the alignment of the solvent dipoles. For the lipid bilayer membranes and the considered mixtures, a study should be performed to verify whether the thermal energy is strong enough to disrupt the reorientation of the solvents.

3. Phase recognition with DII and BNP

It might often be far from obvious to find the proper probe for the requested analysis, as a plethora of probes is available, and more are synthetized every year, with more focused application and less general use. A family of probes which is widely used in experimental characterization of membrane phases is the dialkyl carbocyanine (DiI) one, characterized by emission and absorption transition state dipole moment which coincide with the probe's long axis [27,28]. It is known that indocarbocyanine probes with a linker of three and five carbons have similar membrane properties [29]. Since the probe with the five membered bridge is excited in the red and emits in the far red [30], we focus on this probe only, which is denoted as 1,1′-dioctadecyl-3,3,3′,3′-tetramethylindocarbocyanine (DiI-C18(5), furtheron labelled DiD). As the degree of phototoxicity is far lower for longer excitation wavelengths, and the autofluorescence is reduced, this compound is better suited for experiments on living cells.

Making use of its chemical stability, its bright fluorescence, the subsequent high luminescence quantum yield, and its absorption as well as emission bands in the visible range, the so-called BODIPY compound of Treibs and Kreuzer [31] has been used to create the meso-amino-substituted 8-[(2-sulfonatoethyl)amino]-4,4-difluoro-3,5-dioctadecyl-4-bora-3a,4a-diaza-s-indacene (BNP) probe, which was expected to express similar behaviour in membranes as DiD, but with fluorescence shifted in the blue part of the visible spectrum. In spectrophotometry and fluorescence spectroscopy experiments with membrane mixtures, BNP was found to partitioned preferentially in the same lipid phases as DiD [27]. In this work, both BNP and DiD were studied in DOPC(Ld)/DPPC(So) (2:3) and DOPC/SM/Chol (1:2:1) (Ld/Lo) mixtures, but it was not clear which membrane phase was preferred by either of the two compounds.

Making use of extensive molecular dynamics calculations and the z-constrained method [32], the Gibbs free energy profiles for both BNP and DiD were calculated with bulk water as a reference, with an accuracy of ~1 kcal/mol. The plots for DiD showed that the deepest wells are obtained for the DPPC (So) membrane while the least favourable Gibbs free energy is found for DOPC (Ld) (Fig. 2a). This is confirmed by confocal microscopy images, which show mainly the So and Lo regions in Ld/So and Ld/Lo lipid phase mixtures, respectively. These simulations indicated as well that the chromophore moiety of DiD is located at the surface of the Lo membrane in contact with bulk water, which contrasts strongly with the deeper location of the probe in the other membranes. In fact, in Lo DiD experiences free volumes inducing a small cavity in the membrane in which water molecules are pulled (Fig. 2d). They can be interpreted as notches in the membrane surface. Although the probe might be exposed to the water molecules the closest to the surface, it can be remarked that the probe is still located inside this 2:1 SM/Chol membrane. When cholesterol is added, the fluidity and elasticity of the membrane increases. As formulated in a work based on AFM measurements which states that membrane defects emerge at higher concentrations of Cholesterol [33], this stabilizing effect has been found to trigger the formation of blebs. In our considered model membrane, the free volume or bleb-like structure is consecutively filled with water. The analysis of the molecular dynamics calculations revealed that the position and orientation of the DiD and BNP probes are not equivalent; the chromophore headgroup of BNP exhibits a weak zwitterionic charge distribution between the slightly positive nitrogen and negative boron atoms which allows interactions with water molecules in the proximity of the probe's position in DPPC (So) (Fig. 2b). A similar localization of BNP is found in DOPC and SM/Chol, which results from additional interactions with tails unsaturation and Chol. Unlike DiD, the Gibbs free energy profiles for BNP exhibited markedly small differences between the different profiles. Within the constraints of the performed simulations and used theories, a comparison with DiD was indeed required to explain and identify the confocal microscopy images, which showed the same bright areas for both BNP and DiD probes.

Knowing that cancer cells exhibit increased membrane fluidity and are characterized by a higher polarity compared to healthy cells [34–36], it is of utmost importance to develop and verify the use of non-invasive methods and optical techniques to enable differentiation between healthy and malignant cells. Using molecular modelling and a framework of hybrid QM/MM approaches, non-linear optical spectroscopy, fluorescence anisotropy and fluorescence lifetime imaging can be simulated. In terms of computational cost, the use of a united atom force field was of importance in the calculation of the Gibbs' Free Energy profiles where for each pulling step of 1 Å a MD run of 100 ns was used, but, as a consequence, when optical properties are calculated, attention has to be paid to the correct addition of hydrogen atoms in the backbones of a conjugated molecule like DiD. From our experience, it is advised to inspect automatic procedures based on visualization packages or on the verification of pH values using the Open Babel package [37,38]. An important improvement on the procedures to investigate fluorescent compounds embedded in lipid bilayers has to be done to reparametrize molecular dynamics force fields for the relevant excited state of the probe. This opens the debate about the most reliable method to describe the excited states of the molecule at the QM level. Appropriate benchmarking of TDDFT functionals is needed and when found to be necessary, correlated ab initio methods like coupled cluster theories [39] or the Algebraic Diagrammatic Construction scheme (ADC) [40] should be used. With respect to computational cost and scalability with system size and thanks to their sustained development [41–45], the importance of the latter methods might increase in the field through the next coming years.

For DiD, we proved that the linear and non-linear optical techniques can be used to discriminate between the different membrane phases

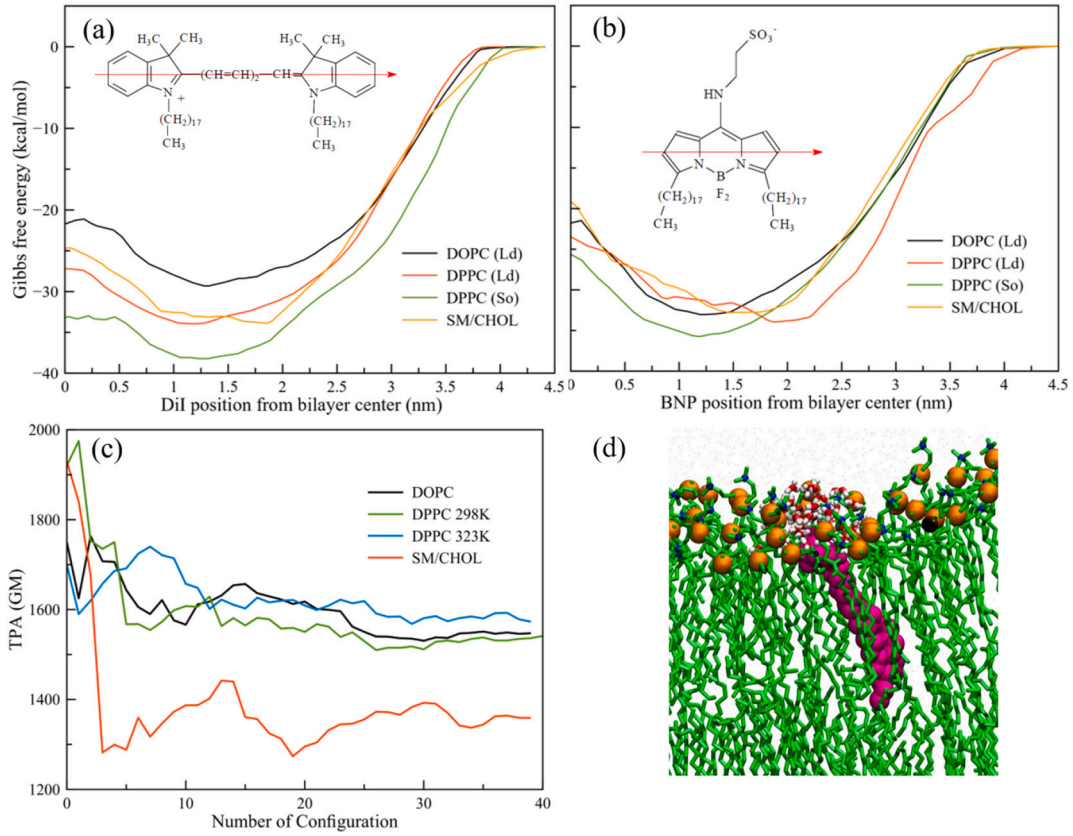

Fig. 2. Gibbs free-energy surfaces of DiD (a) and BNP (b) in function of the distance from the membrane center. The transition dipole moment is reported as a red arrow; (c) two-photon absorption (TPA) cross section of DiD in the different membranes for the S2 excited state; (d) Water molecules in proximity of the DiD probe in the SM/CHOL membrane. The DiD molecule is shown in magenta sticks, water within 8 Å are shown as red and white sticks, phosphates are displayed as orange balls, oxygen of cholesterol as red balls while lipid molecules are shown as green sticks (green – carbon, blue – nitrogen, red – oxygen).

[46]. In OPA, the condition of the biological environment induces different fine structures and energetically different absorption windows. The cross section values in TPA also depend on the lipid phase (Fig. 2c): in the Ld phase they are much higher than in So and even Lo phase. In Lo membrane this is an effect of the particular position on the probe and the presence of water molecules in the immediate neighborhood of the probe (Fig. 2d). For the first hyperpolarizabilities which are decisive in Second Harmonic Generation (SHG) and Hyper Rayleigh Scattering (HRS), clearly expressed relative orders between the phases are seen. Even the simulation of techniques which exhibit the rotational correlation function and the decay of the fluorescence anisotropy of DiD point at the opportunities of these methods which all together can be used as a toolbox for an early detection of aberrant cell structures. In contrast to experimental data which already indicated that the BNP probe cannot be used in a fluorescence lifetime image (FLIM), molecular modelling showed that this is different for DiD, for which FLIM images might be useful to identify lipid bilayer phases, and that DiD can be used as a universal probe in lipid bilayer membranes [46].

Finally, DiD has in general been believed to be an Ld lipid phase marker [29,47–48]. Based on the presented MD and QM/MM calculations, evidence is provided to revise that picture. For a DOPC/SM/Chol (1:2:1) membrane, the probe is found to prefer the Lo SM/Chol lipid bilayer. In addition, the probe is seemingly located in a notch at the upper bound of the membrane, in the immediate vicinity of water molecules, which is important to consider when experimentally obtained optical spectra are interpreted.

4. Azobenzene as novel probe for lipid phase recognition

To demonstrate the predictive capability of modern computational frameworks in a multiscale approach, we refer here to recent studies on azobenzene derivatives for phase recognition. Azobenzene is a photochromic molecule which is widely used in material chemistry for its interesting photoswitching properties, and over the years has been used for many different applications, from cargo lift to switchable components indispensable for on/off OFET devices [49–51]. Despite the wide usage of this molecule, its range of applications in biological environments is rather limited to DNA related studies [52–56], while we are convinced that it can be a very interesting probe for phase recognition, especially when azobenzene's photoswitching activity is exploited.

In this view, we carried out computational studies to assess the feasibility of our assumption, and we started with a canonical azobenzene molecule modified with alkyl chains substituted in the para position of the phenyl rings to ease the insertion in the membrane and enhance the hydrophobic interactions. The chain length was increased from C_2H_5 up to $C_{18}H_{37}$ carbon atoms [57]. The main goal of this study is to assess a priori the effect of alkyl chain lengths on the localization of the probe in a DOPC (Ld) membrane, and what is the effect of cis/trans isomerization on different optical responses. Once more, a multiscale approach is considered, with long MD simulations run on each isomer for each chain length. We found that there is a strong correlation between the localization of the probe and the length of the tails: when the latter one increases, the position of the whole probe in the membrane is strongly affected. For the trans isomer, the strong hydrophobic interaction of the tails leads to a localization of the azobenzene close to the centre of the bilayer, with the chains stretching out parallel to the bilayer tails. In contrast, the cis isomer possesses a strong dipole moment due to the lone pairs on the nitrogen atoms, which results into a strong hydrophilic interaction of the core of the probe with the membrane head group. Interestingly, now the increase in chain length 'pushes' the azo

core toward the membrane surface, rather than 'pulling' it toward the centre as found for the trans isomer. As a result, the azobenzene orients in different ways depending on the nature of the isomer: the trans isomer is slightly tilted with respect to the membrane normal, while the cis is located close to the polar head group with its main axis almost parallel to the membrane surface.

The correlation between the tails and the observed pushing effect for the cis isomers is strongly seen through the non-linear optical (NLO) spectroscopies. The S_2 is the active state in the TPA cross section analysis, with values which increase along with the tail length. In contrast, for the deep lying trans isomer, the pushing effect of the tails lead to TPA cross section values which are unaltered by the environment. The combination of the different push/pull effects is responsible for the high cross section values for the cis isomer, 10 times higher than for the trans. The investigation of the simulated second susceptibility $\chi^{(2)}$, observed in second harmonic generation measurements, shows that the cis isomers have values 10 times higher than the trans ones, irrespective of the tail lengths, making this isomer the active state (Fig. 3a). Thus, harvesting the power of computation, we can assess a priori the versatility of novel probes, which can then be experimentally synthetized and characterized.

To move a step further, we rationally designed a novel azobenzene-based probe, to assess the predictive power of our molecular modelling strategy. The probe consists out of a hexabenzocoronene (HBC) core connected to the azobenzene phenyl ring (HBC-azo) and has been immersed in two different model membranes, DOPC (Ld) and DPPC (So). In this study the focus is to take advantage of the photoswitching properties of the azobenzene to be able to screen between different membrane phases through the presence of "on/off" states depending on the trans/cis isomerization. From MD simulations, we observed different localizations of the two isomers in the membranes considered; although the trans isomer has similar position and orientation in both phases, the cis isomer is more sensitive to the environment, localizing itself at different distances from the bilayer center [58]. Thus, we can already assume that the response to optical stimuli will be different depending on the environment, especially for the cis isomer.

To corroborate our assumption, we performed OPA and TPA analyses by means of QM/MM calculations. As expected, for the trans isomer similar OPA and TPA spectra have been obtained, while the cis isomer is the one which controls the outcome of the optical properties in the lipid bilayers. In DOPC the cis acts as the "on" state for both OPA and TPA properties, while in DPPC, due to its different localization, it is the "off" state. This should translate in different images from TPA microscopy, which can be used to discriminate between different membrane phases.

Similar interpretations of "on/off" states are possible in the fluorescence anisotropy analysis, too. The fluorescence decay time of the HBC-azo conformers in the different phases shows that S_1 is a dark state, while S_2 is the first active state with a decay time of 3.6 (1.8) ns for the cis (trans) in DOPC, while values of 5.4 and 1.1 ns are obtained for the trans and cis isomers in DPPC, respectively (Fig. 3b). It is possible to recognise the two phases by comparing the radiative decay time in DPPC and DOPC. Thus, from these analyses we conclude that computational simulations can recognise different phases using the same isomer, and that, on the other hand, different isomers in the same phase lead to a different response, making such probe versatile for phase detection.

It can be noted that Fig. 3b is based on the emission life time as calculated from the Einstein coefficient for spontaneous emission. This means that effects of non-radiative decay are not included. The presented picture could be significantly improved and even directly compared to experimentally obtained Fluorescent Lifetime Images (FLIMs) if it is multiplied by the quantum yield. To achieve theoretical access to it, surface hopping methodologies and ab initio molecular dynamics calculations on the azobenzene probe embedded in its environment are needed. A promising approach has been developed by Persico and co-workers and is based on semi-classical methods to predict the excited state dynamics of azobenzene derivatives [59,60]. It is based on Tully's few switches algorithm [61] and makes use of floating occupation numbers that depend on the molecular orbital energies.

5. Conclusions and perspectives

In this review, we pinpointed the power of computations to predict and explain the outcome of optical spectroscopies which are often used in experimental biophysical sciences. We proved that extensive molecular dynamics calculations provide profound and necessary insight into their orientation and position in the surrounding lipid bilayer. Through extensive hybrid QM/MM methodologies, one can simulate and analyze (non-) linear optical spectra which are accessible through confocal microscopy images. We focused here especially on three sets of molecular probes for which a deep analysis of the localization and the optical properties revealed new insights into the probes' use and application fields.

The question can be asked which of the compounds would be the most beneficial to discriminate between membrane phases in an experiment based on the non-linear optical effects. The fluorescence anisotropy of conf-II of Laurdan decays strongly for the DOPC (Ld) membrane, while it stays relatively constant in the DPPC (So) one. When TPA is used, the large difference between the cross sections for conf-I and conf-II is conveniently used to identify the So phase: this difference diminishes in Ld phase. Thanks to its particular position mentioned above, DiD on the other hand is the probe of choice when TPA is used to discriminate the investigated Cholesterol mixture in Lo phase from the Ld and So lipid membranes. With respect to the SHG and HRS spectroscopies, conf-II of Laurdan exhibits a larger difference between Ld

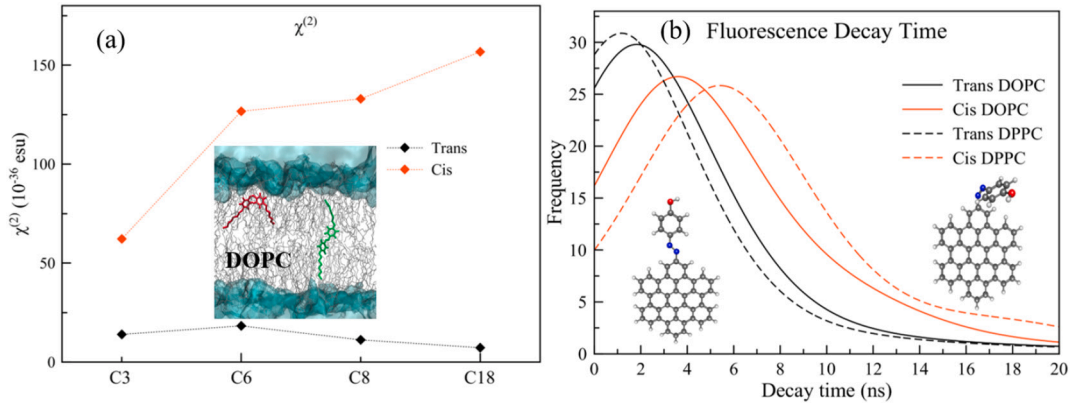

Fig. 3. (a) Second susceptibility analysis in esu units for the TC8 (green structure in the inset) and CC8 (red structure) isomers in DOPC (Ld); (b) Fluorescence decay time for the HBC-azo trans (black lines) and cis (red lines) isomers in the DOPC Ld phase (solid lines) and in DPPC So phase (dashed lines).

and So phase than DiD. Finally, the difference between the second susceptibilities obtained in Ld and So phase for the cis conformer of azobenzene increases profoundly with tail length. Conformationally versatile probes like the azobenzene derivative proposed in this work show that light can be used to tune the active state of the probe for its particular use in a membrane.

With this review article, we hope to trigger the interest of applied spectroscopists, who can use and further develop the revealed characteristics of the probes. The work presented here proves that the deep insights brought by computations can be used together with biophysical experiments to design and set-up research proposals which further excavate the potential of non-linear optical techniques in biomedical applications.

Declaration of competing interest

The authors declare that they have no known competing financial interests or personal relationships that could have appeared to influence the work reported in this paper.

Acknowledgments

SO thankfully acknowledge the financial support from the Polish National Science Centre (grant no. UMO-2018/31/D/ST4/01475); SK gratefully acknowledge the financial support from the Czech Science Foundation (grant no. 17-21122S). For the computational time, the Swedish (SNIC) and Flemish (VSC) national computer infrastructures are acknowledged, along with the Interdisciplinary Center for Mathematical and Computational Modelling (ICM, University of Warsaw) under the GA73-16, GA76-5, and GB80-24 computational grants.

References

[1] K. Berka, M. Paloncyova, P. Anzenbacher, M. Otyepka, Behavior of human cytochromes P450 on lipid membranes, J. Phys. Chem. B 117 (2013) 11556–11564, https://doi.org/10.1021/jp4059559.
[2] P.C. Biggin, M.S.P. Sansom, Interactions of alpha-helices with lipid bilayers: a review of simulation studies, Biophys. Chem. 76 (1999) 161–183, https://doi.org/10.1016/S0301-4622(98)00233-6.
[3] M. Franova, J. Repakova, P. Capkova, J.M. Holopainen, I. Vattulainen, Effects of DPH on DPPC-cholesterol membranes with varying concentrations of cholesterol: from local perturbations to limitations in fluorescence anisotropy experiments, J. Phys. Chem. B 114 (2010) 2704–2711, https://doi.org/10.1021/jp908533x.
[4] M. Hirtz, N. Kumar, L. Chi, Simulation modeling of supported lipid membranes - a review, Curr. Top. Med. Chem. 14 (2014) 617–623, https://doi.org/10.2174/1568026614666140118204332.
[5] P. Kosinova, K. Berka, M. Wykes, M. Otyepka, P. Trouillas, Positioning of antioxidant Quercetin and its metabolites in lipid bilayer membranes: implication for their lipid-peroxidation inhibition, J. Phys. Chem. B 116 (2012) 1309–1318, https://doi.org/10.1021/jp208731g.
[6] A.P. Lyubartsev, A.L. Rabinovich, Recent development in computer simulations of lipid bilayers, Soft Matter 7 (2011) 25–39, https://doi.org/10.1039/c0sm00457j.
[7] M.F. Coughlin, D.R. Bielenberg, G. Lenormand, M. Marinkovic, C.G. Waghorne, B. R. Zetter, J.J. Fredberg, Cytoskeletal stiffness, friction, and fluidity of cancer cell lines with different metastatic potential, Clin Exp Metastasis 30 (2013) 237–250, https://doi.org/10.1007/s10585-012-9531-z.
[8] S. Bhattacharjee, I. Jose, Early detection of breast cancer: a molecular optical imaging approach using novel estrogen conjugate fluorescent dye, in: Optical Tomography and Spectroscopy of Tissue IX, International Society for Optics and Photonics, 2011, p. 78961F, https://doi.org/10.1117/12.873387.
[9] A.P. Demchenko, Y. Mely, G. Duportail, A.S. Klymchenko, Monitoring biophysical properties of lipid membranes by environment-sensitive fluorescent probes, Biophys. J. 96 (2009) 3461–3470, https://doi.org/10.1016/j.bpj.2009.02.012.
[10] J. Kongsted, A. Osted, K.V. Mikkelsen, O. Christiansen, The QM/MM approach for wavefunctions, energies and response functions within self-consistent field and coupled cluster theories, Mol. Phys. 100 (2002) 1813–1828, https://doi.org/10.1080/00268970110117106.
[11] A.S. Klymchenko, R. Kreder, Fluorescent probes for lipid rafts: from model membranes to living cells, Chem. Biol. 21 (2014) 97–113, https://doi.org/10.1016/j.chembiol.2013.11.009.
[12] S. Osella, S. Knippenberg, Laurdan as a molecular rotor in biological environments, ACS Appl Bio Mater 2 (2019) 5769–5778, https://doi.org/10.1021/acsabm.9b00789.
[13] S. Osella, N.A. Murugan, N.K. Jena, S. Knippenberg, Investigation into biological environments through (non)linear optics: a multiscale study of Laurdan derivatives, J. Chem. Theory Comput. 12 (2016) 6169–6181, https://doi.org/10.1021/acs.jctc.6b00906.
[14] L. Bagatolli, E. Gratton, T.K. Khan, P.L.G. Chong, Two-photon fluorescence microscopy studies of bipolar tetraether giant liposomes from thermoacidophilic archaebacteria Sulfolobus acidocaldarius, Biophys. J. 79 (2000) 416–425, https://doi.org/10.1016/S0006-3495(00)76303-X.
[15] L.A. Bagatolli, E. Gratton, Direct observation of lipid domains in free-standing bilayers using two-photon excitation fluorescence microscopy, J. Fluoresc. 11 (2001) 141–160, https://doi.org/10.1023/A:1012228631693.
[16] J. Barucha-Kraszewska, S. Kraszewski, C. Ramseyer, Will C-Laurdan dethrone Laurdan in fluorescent solvent relaxation techniques for lipid membrane studies? Langmuir. 29 (2013) 1174–1182, https://doi.org/10.1021/la304235r.
[17] E. Gibbons, K.R. Pickett, M.C. Streeter, A.O. Warcup, J. Nelson, A.M. Judd, J. D. Bell, Molecular details of membrane fluidity changes during apoptosis and relationship to phospholipase A(2) activity, Biochim Biophys Acta-Biomembr 1828 (2013) 887–895, https://doi.org/10.1016/j.bbamem.2012.08.024.
[18] A.G. Jay, J.A. Hamilton, Disorder amidst membrane order: standardizing Laurdan generalized polarization and membrane fluidity terms, J. Fluoresc. 27 (2017) 243–249, https://doi.org/10.1007/s10895-016-1951-8.
[19] S.S.W. Leung, J. Thewalt, Link between fluorescent probe partitioning and molecular order of liquid ordered-liquid disordered membranes, J. Phys. Chem. B 121 (2017) 1176–1185, https://doi.org/10.1021/acs.jpcb.6b09325.
[20] H. Tanaka, S. Oasa, M. Kinjo, K. Tange, Y. Nakai, H. Harashima, H. Akita, Temperature and pH sensitivity of a stabilized self-nanoemulsion formed using an ionizable lipid-like material via an oil-to-surfactant transition, Colloid Surf B-Biointerfaces. 151 (2017) 95–101, https://doi.org/10.1016/j.colsurfb.2016.11.020.
[21] H.M. Kim, H.-J. Choo, S.-Y. Jung, Y.-G. Ko, W.-H. Park, S.-J. Jeon, C.H. Kim, T. Joo, B.R. Cho, A two-photon fluorescent probe for lipid raft imaging: C-Laurdan, ChemBioChem 8 (2007) 553–559, https://doi.org/10.1002/cbic.200700003.
[22] S. Osella, N. Smisdom, M. Ameloot, S. Knippenberg, Conformational changes as driving force for phase recognition: the case of Laurdan, Langmuir 35 (2019) 11471–11481, https://doi.org/10.1021/acs.langmuir.9b01840.
[23] H. Sumi, Theory on reaction rates in nonthermalized steady states during conformational fluctuations in viscous solvents, J. Phys. Chem. 95 (1991) 3334–3350, https://doi.org/10.1021/j100161a068.
[24] T. Asano, Kinetics in highly viscous solutions: dynamic solvent effects in “slow” reactions, Pure Appl. Chem. 71 (1999) 1691–1704, https://doi.org/10.1351/pac199971091691.
[25] S. Baral, M. Phillips, H. Yan, J. Avenso, L. Gundlach, B. Baumeier, E. Lyman, Ultrafast formation of the charge transfer state of Prodan reveals unique aspects of the chromophore environment, J. Phys. Chem. B 124 (2020) 2643–2651, https://doi.org/10.1021/acs.jpcb.0c00121.
[26] Lakowicz, Principles of Fluorescence Spectroscopy, 3rd edition, Springer, 2007.
[27] M. Bacalum, L. Wang, S. Boodts, P. Yuan, V. Leen, N. Smisdom, E. Fron, S. Knippenberg, G. Fabre, P. Trouillas, D. Beljonne, W. Dehaen, N. Boens, M. Ameloot, A blue-light-emitting BODIPY probe for lipid membranes, Langmuir 32 (2016) 3495–3505, https://doi.org/10.1021/acs.langmuir.6b00478.
[28] S. Knippenberg, G. Fabre, S. Osella, F. Di Meo, M. Paloncyova, M. Ameloot, P. Trouillas, Atomistic picture of fluorescent probes with hydrocarbon tails in lipid bilayer membranes: an investigation of selective affinities and fluorescent anisotropies in different environmental phases, Langmuir 34 (2018) 9072–9084, https://doi.org/10.1021/acs.langmuir.8b01164.
[29] D. Scherfeld, N. Kahya, P. Schwille, Lipid dynamics and domain formation in model membranes composed of ternary mixtures of unsaturated and saturated phosphatidylcholines and cholesterol, Biophys. J. 85 (2003) 3758–3768.
[30] K. Bacia, D. Scherfeld, N. Kahya, P. Schwille, Fluorescence correlation spectroscopy relates rafts in model and native membranes, Biophys. J. 87 (2004) 1034–1043, https://doi.org/10.1529/biophysj.104.040519.
[31] A. Treibs, F.-H. Kreuzer, Justus Liebigs Ann Chem 718 (1968) 208.
[32] M. Paloncyova, K. Berka, M. Otyepka, Convergence of free energy profile of coumarin in lipid bilayer, J. Chem. Theory Comput. 8 (2012) 1200–1211, https://doi.org/10.1021/ct2009208.
[33] C. Lamprecht, M. Gehrmann, J. Madl, W. Römer, G. Multhoff, A. Ebner, Molecular AFM imaging of Hsp70-1A association with dipalmitoyl phosphatidylserine reveals membrane blebbing in the presence of cholesterol, Cell Stress and Chaperones 23 (2018) 673–683, https://doi.org/10.1007/s12192-018-0879-0.
[34] I. Nakazawa, M. Iwaizumi, A role of the cancer cell-membrane fluidity in the cancer metastases, Tohoku J. Exp. Med. 157 (1989) 193–198, https://doi.org/10.1620/tjem.157.193.
[35] I. Nakazawa, M. Iwaizumi, A correlation between cancer metastases and the fluidity of cancer cell-membrane, Tohoku J. Exp. Med. 137 (1982) 325–328, https://doi.org/10.1620/tjem.137.325.
[36] C. Haendel, B.U.S. Schmidt, J. Schiller, U. Dietrich, T. Moehn, T.R. Kiessling, S. Pawlizak, A.W. Fritsch, L.-C. Horn, S. Briest, M. Hoeckel, M. Zink, J.A. Kaes, Cell membrane softening in human breast and cervical cancer cells, New J. Phys. 17 (2015) 083008, https://doi.org/10.1088/1367-2630/17/8/083008.
[37] N.M. O’Boyle, M. Banck, C.A. James, C. Morley, T. Vandermeersch, G. R. Hutchison, Open babel: an open chemical toolbox, J Cheminformatics. 3 (2011) 33, https://doi.org/10.1186/1758-2946-3-33.
[38] The open babel package, version 2.3.1. http://openbabel.org.
[39] T.D. Crawford, H.F. Schaefer, An introduction to coupled cluster theory for computational chemists, in: Reviews in Computational Chemistry, John Wiley & Sons, Ltd, 2007, pp. 33–136, https://doi.org/10.1002/9780470125915.ch2.

[40] A. Dreuw, M. Wormit, The algebraic diagrammatic construction scheme for the polarization propagator for the calculation of excited states, Wiley Interdiscip Rev-Comput Mol Sci 5 (2015) 82–95, https://doi.org/10.1002/wcms.1206.
[41] S. Prager, A. Zech, T.A. Wesolowski, A. Dreuw, Implementation and application of the frozen density embedding theory with the algebraic diagrammatic construction scheme for the polarization propagator up to third order, J. Chem. Theory Comput. 13 (2017) 4711–4725, https://doi.org/10.1021/acs.jctc.7b00461.
[42] M. Scheurer, M.F. Herbst, P. Reinholdt, J.M.H. Olsen, A. Dreuw, J. Kongsted, Polarizable embedding combined with the algebraic diagrammatic construction: tackling excited states in biomolecular systems, J. Chem. Theory Comput. 14 (2018) 4870–4883, https://doi.org/10.1021/acs.jctc.8b00576.
[43] D.R. Rehn, A. Dreuw, Analytic nuclear gradients of the algebraic-diagrammatic construction scheme for the polarization propagator up to third order of perturbation theory, J. Chem. Phys. 150 (2019) 174110, https://doi.org/10.1063/1.5085117.
[44] D. Hrsak, J.M.H. Olsen, J. Kongsted, Polarizable density embedding coupled cluster method, J. Chem. Theory Comput. 14 (2018) 1351–1360, https://doi.org/10.1021/acs.jctc.7b01153.
[45] T. Kjaergaard, P. Baudin, D. Bykov, K. Kristensen, P. Jorgensen, The divide-expand-consolidate coupled cluster scheme, Wiley Interdiscip Rev-Comput Mol Sci 7 (2017) e1319, https://doi.org/10.1002/wcms.1319.
[46] S. Osella, F. Di Meo, N.A. Murugan, G. Fabre, M. Ameloot, P. Trouillas, S. Knippenberg, Combining (non)linear optical and fluorescence analysis of DiD to enhance lipid phase recognition, J. Chem. Theory Comput. 14 (2018) 5350–5359, https://doi.org/10.1021/acs.jctc.8b00553.
[47] N. Kahya, D. Scherfeld, K. Bacia, B. Poolman, P. Schwille, Probing lipid mobility of raft-exhibiting model membranes by fluorescence correlation spectroscopy, J. Biol. Chem. 278 (2003) 28109–28115, https://doi.org/10.1074/jbc.M302969200.
[48] J. Juhasz, J.H. Davis, F.J. Sharom, Fluorescent probe partitioning in giant unilamellar vesicles of “lipid raft” mixtures, Biochem. J. 430 (2010) 415–423, https://doi.org/10.1042/Bj20100516.
[49] N. Crivillers, S. Osella, C. Van Dyck, G.M. Lazzerini, D. Cornil, A. Liscio, F. Di Stasio, S. Mian, O. Fenwick, F. Reinders, M. Neuburger, E. Treossi, M. Mayor, V. Palermo, F. Cacialli, J. Cornil, P. Samori, Large work function shift of gold induced by a novel perfluorinated azobenzene-based self-assembled monolayer, Adv. Mater. 25 (2013) 432–436, https://doi.org/10.1002/adma.201201737.
[50] M. Doebbelin, A. Ciesielski, S. Haar, S. Osella, M. Bruna, A. Minoia, L. Grisanti, T. Mosciatti, F. Richard, E.A. Prasetyanto, L. De Cola, V. Palermo, R. Mazzaro, V. Morandi, R. Lazzaroni, A.C. Ferrari, D. Beljonne, P. Samori, Light-enhanced liquid-phase exfoliation and current photoswitching in graphene-azobenzene composites, Nat. Commun. 7 (2016) 11090, https://doi.org/10.1038/ncomms11090.
[51] J.M. Mativetsky, G. Pace, M. Elbing, M.A. Rampi, M. Mayor, P. Samori, Azobenzenes as light-controlled molecular electronic switches in nanoscale metal-molecule-metal junctions, J. Am. Chem. Soc. 130 (2008), https://doi.org/10.1021/ja8018093, 9192-+.
[52] I.N. Unksov, N.A. Kasyanenko, Conformational changes in the DNA molecule in solution caused by the binding of a light-sensitive cationic surfactant, J. Struct. Chem. 58 (2017) 413–419, https://doi.org/10.1134/S0022476617020287.
[53] N. Kasyanenko, L. Lysyakova, R. Ramazanov, A. Nesterenko, I. Yaroshevich, E. Titov, G. Alexeev, A. Lezov, I. Unksov, Conformational and phase transitions in DNA-photosensitive surfactant solutions: experiment and modeling, Biopolymers 103 (2015) 109–122, https://doi.org/10.1002/bip.22575.
[54] D. Rastaedter, M. Biswas, I. Burghardt, Molecular dynamics study of the controlled destabilization of an RNA hairpin structure by a covalently attached azobenzene switch, J. Phys. Chem. B 118 (2014) 8478–8488, https://doi.org/10.1021/jp501399k.
[55] M. McCullagh, I. Franco, M.A. Ratner, G.C. Schatz, Defects in DNA: lessons from molecular motor design, J. Phys. Chem. Lett. 3 (2012) 689–693, https://doi.org/10.1021/jz201649k.
[56] L. Wu, K. Koumoto, N. Sugimoto, Reversible stability switching of a hairpin DNA via a photo-responsive linker unit, Chem. Commun. (2009) 1915–1917, https://doi.org/10.1039/b819643e.
[57] S. Knippenberg, S. Osella, Push/Pull Effect as Driving Force for Different Optical Responses of Azobenzene in a Biological Environment, review, 2020.
[58] S. Osella, S. Knippenberg, Triggering on/off states of photoswitchable probes in biological environments, J. Am. Chem. Soc. (2017) 4418–4428.
[59] T. Cusati, G. Granucci, M. Persico, Photodynamics and time-resolved fluorescence of azobenzene in solution: a mixed quantum-classical simulation, J. Am. Chem. Soc. 133 (2011) 5109–5123, https://doi.org/10.1021/ja1113529.
[60] G. Granucci, M. Persico, Excited state dynamics with the direct trajectory surface hopping method: azobenzene and its derivatives as a case study, Theor Chem Account 117 (2007) 1131–1143, https://doi.org/10.1007/s00214-006-0222-1.
[61] J.C. Tully, Mixed quantum-classical dynamics, Faraday Discuss. 110 (1998) 407–419, https://doi.org/10.1039/a801824c.